

Caraka Tani: Journal of Sustainable Agriculture, 40(4), 575-591, 2025

URL: https://jurnal.uns.ac.id/carakatani/article/view/107085

DOI: http://dx.doi.org/10.20961/carakatani.v40i4.107085



The Efficiency of Cokriging Spatial Interpolation to Estimate the Electrical Conductivity of Saturated Paste Extract (EC_e) Using Soil to Water Ratios

Koddam Rukadi, Porntip Phontusang* and Anongnat Sriprachote

Department of Soil Science and Environment, Faculty of Agriculture, Khon Kaen University, Khon Kaen, Thailand

*Corresponding author: porntph@kku.ac.th

Abstract

Accurate assessment of soil salinity is essential for managing salt-affected soils and sustaining agricultural productivity. This study evaluated the potential of cokriging spatial interpolation for estimating the electrical conductivity of saturated paste extract (EC_e), using soil electrical conductivity (EC) measured at 1:2.5 and 1:5 soil-to-water ratios. The objectives included identifying suitable scatter plot and cross-variogram models and assessing mapping accuracy. A total of 300 topsoil samples (0 to 30 cm) were collected from three salt-affected soil classes in Muang Pia Sub-district, Khon Kaen Province, Northeastern Thailand. Spatial modelling and cross-variogram analyses were performed using GS+ software to evaluate estimation accuracy across different sample sizes. The results showed that EC measurements at a 1:5 ratio exhibited the strongest correlation with EC_e across all soil classes, with coefficient of determination (R²) values reaching 0.98 in Class 1 and Class 2, and 0.85 in Class 3, despite a minimum sample size (n = 25). Gaussian and spherical models best described these relationships. Higher R² values were consistently associated with lower mean error (ME) and root mean square error (RMSE), in almost all sample sizes and classes, indicating the robustness and reliability of the model across varying salinity conditions. Larger sample sizes (n = 100) yielded more consistent estimation performance, while smaller sample sizes maintained acceptable accuracy, particularly for EC 1:5. This study indicates that soil EC water ratios, especially 1:5, can serve as practical surrogates for EC_e estimation using cokriging spatial interpolation. The proposed approach offers a cost-effective solution for salinity mapping in salt-affected soil areas, with implications for soil monitoring, land management, and sustainable agriculture under limited sampling conditions.

Keywords: digital soil mapping; Northeast Thailand; salt-affected soils; soil water ratios; spatial variability

Cite this as: Rukadi, K., Phontusang, P., & Sriprachote, A. (2025). The Efficiency of Cokriging Spatial Interpolation to Estimate the Electrical Conductivity of Saturated Paste Extract (EC_e) Using Soil to Water Ratios. *Caraka Tani: Journal of Sustainable Agriculture*, 40(4), 575-591. doi: http://dx.doi.org/10.20961/carakatani. v40i4.107085

INTRODUCTION

The study of salt-affected soils is an important topic that encompasses several detrimental effects on arid and semi-arid environments, as many crops are sensitive to high salt concentrations in the soil solution (Qadir et al., 2006; Li et al., 2014; Gozukara et al., 2022). The accumulation of soluble salts in soil adversely affects plant growth,

decreases crop yields, and can lead to total crop failure (Sonmez et al., 2008; Corwin and Yemoto, 2020). Globally, salt-affected soils cover about 7% of the Earth's land area, creating major challenges for sustainable agriculture (Corwin and Yemoto, 2020). The development of salt-affected soils is influenced by natural factors,

^{*} Received for publication July 29, 2025 Accepted after corrections October 23, 2025

such as geological sedimentation and erosion, as well as human activities, including poor irrigation practices, deforestation, shallow groundwater levels, and salt production (Sonmez et al., 2008; Abdelaal et al., 2021).

In Thailand. salt-affected soils are predominantly found in the northeastern region, affecting approximately 2.8 million ha, or roughly 17 to 30% of the land area (Sukchan, 2005; Leksungnoen et al., 2018; Phontusang et al., 2018). These salt-affected soils are caused by both natural factors, particularly the presence of rock salt deposits from the Maha Sarakham Formation (Mitsuchi et al., 1986; Phontusang et al., 2018), and human activities such as irrigation, construction, improper road deforestation, and poorly designed reservoirs (Iwai et al., 2012). Deforestation, often resulting from agricultural expansion, exacerbates salinity by increasing evaporation and promoting the upward movement of salts to the soil surface (Leksungnoen et al., 2018).

The soil electrical conductivity of saturated paste extract (EC_e) is widely regarded as the standard indicator for assessing soil salinity (United States Salinity Laboratory Staff, 1954; Sonmez et al., 2008). However, measuring soil ECe is labor-intensive, costly, and timeconsuming (Matthees et al., 2017; Kargas et al., 2020). In contrast, using soil-to-water ratios, such as 1:2.5 and 1:5, provides a simpler and more economical alternative for estimating salinity (Sonmez et al., 2008; He et al., 2013; Kargas et al., 2020; Smagin et al., 2024). Studies have shown a significant linear correlation between soil EC_e and soil electrical conductivity (EC) measured from water suspensions, although the latter generally underestimates EC_e values (Sonmez et al., 2008; Chi and Wang, 2009; He et al., 2013; Shahid et al., 2018; Corwin and Yemoto, 2020; Kargas et al., 2020).

Spatial variability analysis using geostatistical techniques enables the estimation of soil properties in unsampled locations. Kriging has been frequently used to map EC_e variability; however, it does not incorporate any information about the correlation between different methods (secondary variables) as conducted Phontusang et al. (2018). Normally, the linear regression is used with basic statistics to establish the relationship between two variables; nevertheless, there is no spatial correlation between EC_e and soil EC water ratios, as conducted by Rukadi et al. (2025). Cokriging, on the other hand, leverages the correlation between primary (EC_e) and secondary (EC water ratios) variables, enhancing the spatial prediction of EC_e (Yang et al., 2021). It is advantageous in large-scale mapping where laboratory analysis is limited by time and laboratory resources (Abdelaal et al., 2021; Hossen et al., 2022).

Sample size significantly influences the reliability of predictive models in soil salinity studies. Although larger sample sizes enhance prediction accuracy, smaller samples may still offer practical insights under constrained conditions (Or, 2010; Phontusang et al., 2017). Despite the potential of EC_e estimation from EC water ratios, no studies have applied cokriging to map spatial variability in different salt-affected soil class areas using varying sample sizes and soil EC water ratios.

Therefore, this study aimed to evaluate the spatial variability of EC_e in salt-affected soils in Northeast Thailand by applying the cokriging method using soil EC water ratios of 1:2.5 and 1:5 data across different sample sizes. The specific objectives were to identify suitable scatter plot models and cross-variogram models for EC_e estimation and to assess the mapping accuracy of EC_e from EC water ratios data using the cokriging method.

MATERIALS AND METHOD

Research location and soil sampling

The research location is situated in the inland areas of Muang Pia Sub-district, covering approximately 73.40 km² and consisting of 14 villages. The primary land use is agricultural, with rice cultivation being the main crop (Muang Pia Sub-district, 2022), as indicated in Figure 1. In particular, the southern and western parts of the sub-district are characterized by hills interspersed with plains, which are used for agriculture and horticulture. The eastern and southern regions are dominated by lowland rice fields, while the northern region is predominantly saline and supports limited vegetation, mostly halophytes. Historically, the saline areas in the north have been used for small-scale salt production.

The climate in the region is tropical monsoon. The rainy season occurs from May to September, with average temperatures between 20 to 25 °C and an annual precipitation of approximately 1,196 mm (Weather and climate, 2025). High rainfall during this season may temporarily improve soil quality by leaching salts beyond the root zone. The summer season spans from February to April, with peak temperatures of

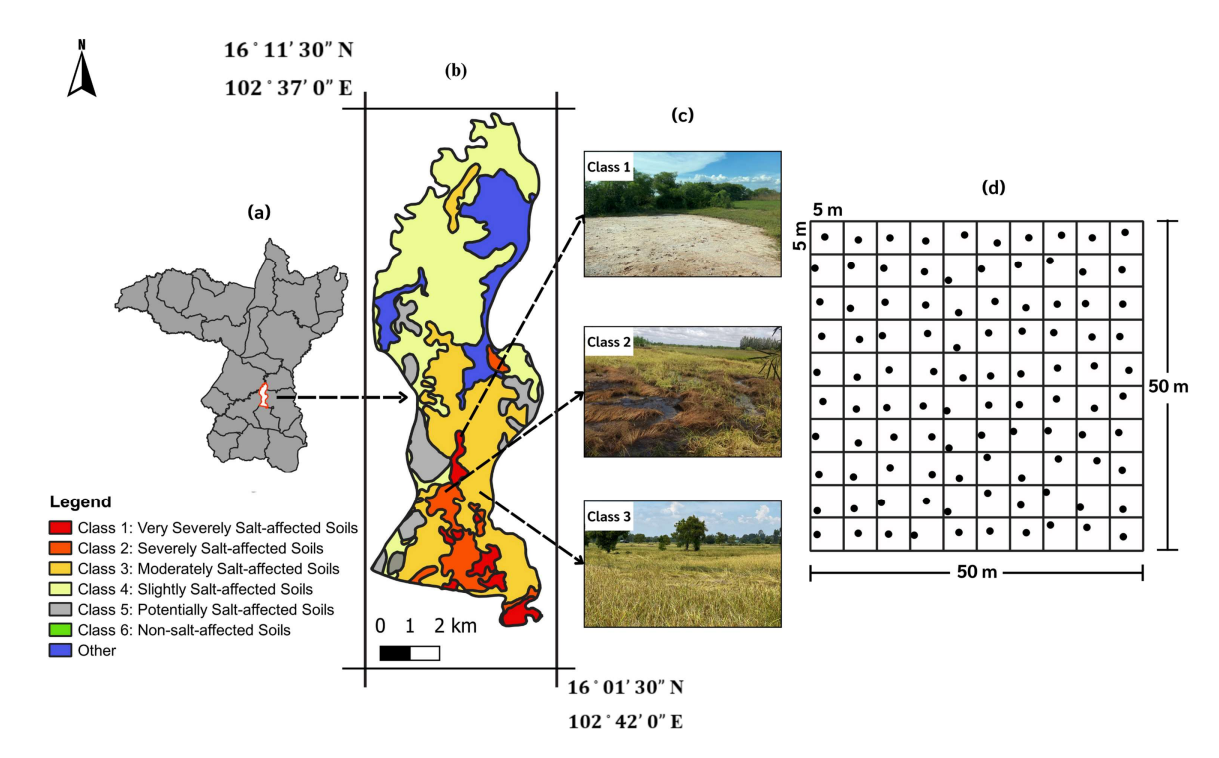


Figure 1. The geographic locations of the study area. (a) Khon Kaen Province, (b) Muang Pia Sub-district with salt-affected soils class, (c) study sites based on different degrees of salt-affected soils classes, and (d) grid sampling points (n = 100) represent soil samples collected based on the stratified systematic unaligned sampling using $50 \text{ m} \times 50 \text{ m}$ of representative area in an equivalent grid measuring $5 \text{ m} \times 5 \text{ m}$

35 to 37 °C, which enhance evaporation and promote salt accumulation on the surface. The winter season lasts from October to January, with temperatures ranging from 14 to 15 °C. Although lower temperatures may reduce evaporation, limited rainfall during winter may contribute to long-term salinity problems (Muang Pia Subdistrict, 2022).

Soil sampling was conducted during the dry season based on the percentage of surface salt crust, following the classification method of Wichaidit (1995). The same sampling locations and soil samples as reported by Phontusang et al. (2017) were used. The study area was classified into three salt-affected classes (Classes 1 to 3) based on visible salt crust coverage and vegetation. Specifically, Class 1 is categorized as very severely salt-affected soils, where > 50% of the soil surface exhibited salt crusts. This class supports only highly salt-tolerant species such as Puccinellia tenuiflora, Acacia salicina, Sporobolus cryptandrus, and Azima sarmentosa (Blume) Benth & Hook. F., which possesses the ability to thrive under these conditions. The occurrence of Azima sarmentosa (Blume) Benth & Hook. F. serves as a bioindicator of saline soils (Sankla et al., 2022). Furthermore, Class 1 is classified

as loam soil texture, with particle-size distribution of 44.96% sand, 35.78% silt, and 19.26% clay. Despite being loamy, which is generally favorable for plant growth (Thanh et al., 2022; Khanh et al., 2024), the high salinity in this class severely restricts agricultural productivity.

Class 2 is classified as severely salt-affected soils where 10 to 50% of the soil surface is covered with salt crusts. This class supports a variety of plant species, including *Oryza sativa*, *Psidium guajava*, and *Capsicum annuum*. However, spatial heterogeneity exists, with some areas unsuitable for plant growth due to localized high salinity (Figure 1). The soil texture is sandy loam, with particle-size distribution of 53.38% sand, 31.06% silt, and 15.56% clay. Although sandy loam provides good fertility, structure, and water retention (Daneshvar et al., 2024), salt stress remains a limiting factor in parts of this class.

Class 3 is classified as moderately salt-affected soils with 1 to 10% surface salt crusts. This class is characterized by a clay loam soil texture, with particle-size distribution of 40.88% sand, 29.11% silt, and 30.01% clay. Moreover, the relatively low salinity levels in this class support more favorable conditions for cultivation. The high sand content in clay loam enhances adsorption

capacity and ease of tillage, making it suitable for diverse crops (Qi et al., 2021). Note that the soil texture measurements were obtained as general representations of each salt-affected soil class based on salt crust surface percentage.

A total of 300 topsoil samples (0 to 30 cm depth) were collected, with 100 samples representing each salt-affected class. Sampling was conducted using a stratified systematic unaligned method. For each class, a representative $50 \text{ m} \times 50 \text{ m}$ (around 0.25 ha) area was delineated and subdivided into a $5 \text{ m} \times 5 \text{ m}$ grid (Figure 2), from which one sample per grid was randomly selected (n = 100). All samples were air-dried at room temperature and stored in labeled ziploc bags. The samples were subsequently transported to the Soil Science and Environment Laboratory, Faculty of Agriculture, Khon Kaen University, for analysis of soil EC using different soil-to-water ratios.

Soil EC water ratios analyses

Soil EC measurements at water ratios of 1:2.5 and 1:5 were conducted following the methodology described by the United States Salinity Laboratory Staff (1954). The soil samples used in this study were derived from the dataset previously collected by Phontusang et al. (2017). A total of 300 air-dried soil samples were analyzed for each water ratio. For the 1:2.5 ratio, 20 g of air-dried soil was mixed with 50 ml of distilled water. The soil water suspension was manually stirred for 10 minutes, and then allowed equilibrate for 30 minutes before EC measurement using a calibrated EC meter. The 30-minute period was selected based on findings by He et al. (2012), which indicated that this duration is generally sufficient for most soils to reach a stable EC value. The procedure for the EC 1:5 ratio followed the same method, with 20 g of air-dried soil and 100 ml of distilled water under identical conditions of beaker glass size, mixing time, equilibrium duration, and temperature. Furthermore, soil textural analysis for both soil EC water ratios has been tested using the pipette method (Gee and Or, 2002). The soil EC $_{\rm e}$, considered the reference salinity parameter, was also obtained from the data reported in Phontusang et al. (2017).

Soil samples selection for EC_e estimation

Soil samples selection for the estimation of ECe was based on the comparison between measured EC_e values and corresponding soil EC values determined from both soil-to-water ratios. To evaluate the influence of sample sizes on estimation accuracy, three sample sizes; 25, 50, and 100, were selected using a systematic grid sampling approach (Figure 2). The sample size of 25 was recommended by Phontusang et al. (2017) who suggested that a minimum sampling density of ≥ 1 sample per 5 m \times 5 m area is appropriate for a field size of $\geq 50 \text{ m} \times 50 \text{ m}$, corresponding to 25 sampling points. For the 25-sample dataset, samples were selected by systematically removing 3 of every 4 sampling points from the original 100-sample grid. For the 50-sample dataset, 2 of every 4 sampling points were removed. The 100-sample dataset represents the full sampling grid with no points removed. stratified reduction method consistent spatial coverage across sample sizes and allowed for comparison in evaluating the impact of sampling density on EC_e estimation.

To develop the cokriging model for estimating EC_e, cross-variogram analyses were conducted between EC_e and soil EC values obtained from 1:2.5 and 1:5 water ratios across varying sample sizes (25, 50, and 100). A total of 18 datasets were generated (Table 1) to assess the spatial

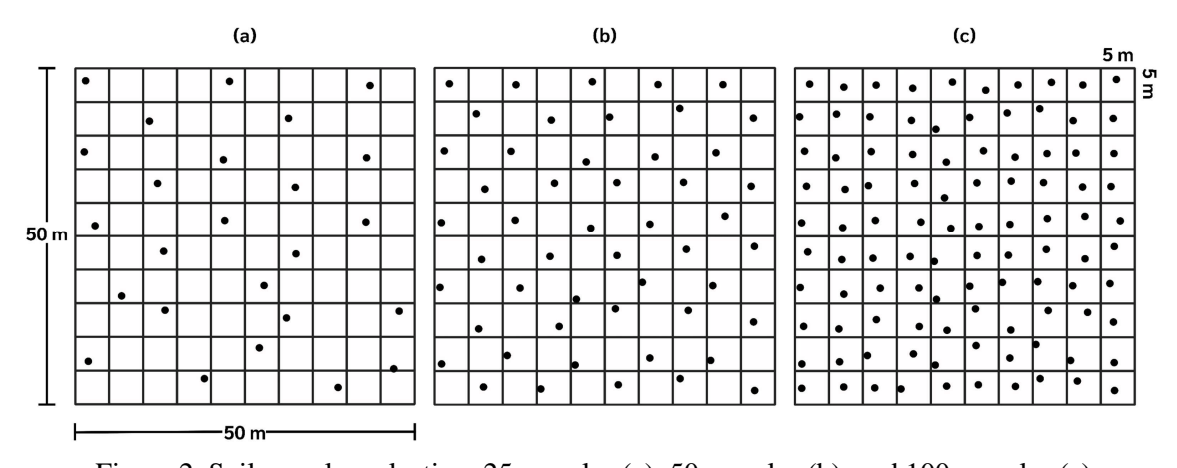


Figure 2. Soil samples selection, 25 samples (a), 50 samples (b), and 100 samples (c)

Table 1. Bolt samples selection of ECe and EC water ratios						
Class	Dataset number	$EC_e \times EC 1:2.5$	Dataset number	$EC_e \times EC 1:5$		
1	1	25×25	10	25×25		
	2	50×50	11	50×50		
	3	100×100	12	100×100		
2	4	25×25	13	25×25		
	5	50×50	14	50×50		
	6	100×100	15	100×100		
3	7	25×25	16	25×25		
	8	50×50	17	50×50		
	9	100×100	18	100×100		

Table 1. Soil samples selection of EC_e and EC water ratios

correlation between EC_e and each EC water ratio. The most suitable cross-variogram model for each combination was selected based on best-fit criteria and used to validate the estimation performance of EC_e in limited sample sizes. This approach demonstrates that reliable estimation is achievable even under reduced sampling densities, supporting the applicability of cokriging in salt-affected soil mapping.

Soil EC_e classification

In this study, salt-affected soils were classified based on salt crust surface percentage following the criteria of Wichaidit (1995) (Figure 1), while salinity levels were categorized using the EC of the EC_e according to the classification proposed by Plaster (2013) (Table 2).

Statistical and geostatistical analysis

In this study, an analysis of skewness was conducted to determine the normality of the original soil EC water ratios data. The skewed (non-normal distribution) datasets characterized by pronounced skewness (skewness > 1 or < -1) were log-transformed prior to geostatistical analysis to enhance the robustness and reliability of the results (Webster and Oliver, 2007). In general, datasets in Class 1 did not require log-transforming, whereas those in Classes 2 and 3 did.

Geostatistical analysis refers to a spatial statistical method based on basic statistics and the concept of regionalized data. The coefficient of variation (CV) is commonly used to assess the degree of variation in soil properties (Lv et al., 2013). The CV is calculated as the ratio of the standard deviation (SD) to the mean (Equation 1). According to the classification by Lv et al. (2013), variation is considered weak, moderate, and strong if the values of CV < 0.10, 0.10 to 1.0, and > 1, respectively.

In addition, the cross-variogram was employed as the principal geostatistical tool to characterize

Table 2. The soil EC_e classification

Code	Salinity class	EC_e (dS m ⁻¹)	
1	Very strongly saline	> 16	
2	Strongly saline	> 8–16	
3	Moderately	> 4–8	
4	Slightly saline	$\geq 2-4$	
5	Non-saline	< 2	

the spatial dependence and variability of EC_e in relation to soil EC values derived from two water ratios. The cross-variogram was calculated using the formulation described by Yates and Warrick (2002) (Equation 2).

The cross-variogram modeling revealed the spatial correlation between the primary (EC_e) and secondary variables (EC), which can be either positive or negative (Seo et al., 2022; Thanh et al., 2022). A negative cross-variogram reflects a negative spatial correlation between the two variables (Spielvogel et al., 2016). It should be noted that the coefficient of determination (R²) remains a positive value, even when a negative spatial correlation exists between variables.

A combined visual assessment and statistical evaluation using the ordinary least squares method was applied to test several standard spherical. models, including exponential, and Gaussian (Marchetti et al., 2012). The effectiveness of the cross-variogram model was evaluated using the R² (Equation 3). The model with the highest R² value was considered the best fit. This parameter was used to assess both the cross-variogram fitting accuracy and the interpolation performance of the cokriging method (Wu et al., 2025). The performance of R² values is presented in Table 3 (Li et al., 2016). Additionally, analysis of variance (ANOVA) was conducted to compare the effects of sample size on the relationship between ECe and EC values across all salt-affected soil classes. Statistical analyses were performed using IBM SPSS Statistics version 28.0.

The best-fit cross-variogram models were characterized by key geostatistical parameters, including the nugget, sill, and range. These primary parameters were used to describe the spatial structure of the variables. In addition, the nugget:sill ratio was calculated to evaluate the degree of spatial dependence, representing the proportion of random variability relative to total spatial variability (Wu et al., 2025). According to Cambardella et al. (1994), nugget:sill ratio values less than 0.25, between 0.25 and 0.75, and greater than 0.75 were categorized as indicating strong, moderate, and weak spatial dependence, respectively. It should be noted that for Gaussian and spherical models, a true range value is not explicitly defined; instead, the "range of influence" is used to describe the distance over which spatial correlation persists (Clark and Harper, 2007). These models have been reported to fit soil property data effectively in various studies (Webster and Oliver, 2007; Wu et al., 2025).

Cokriging analysis

Cokriging is a geostatistical interpolation method used to estimate a primary variable by incorporating one or more secondary variables that are spatially correlated (Yang et al., 2021). The cokriging estimator (Equation 4), as described by Goovaerts (1997), can be applied using various theoretical models, including Gaussian, spherical, and exponential models (Marchetti et al., 2012). In this study, cokriging was employed due to the lack of spatial correlation between EC_e and EC water ratios when analyzed using conventional linear

$$CV = -\frac{\sigma}{\mu}$$
 (1)

Where σ is the SD and μ is the average value of the data (mean).

$$\gamma_{1,2}(h) = \frac{1}{2N(h)} \sum_{i=1}^{N(h)} [z_1(x_i) - z_1(x_i + h)] [z_2(x_i) - z_2(x_i + h)]$$
(2)

Where $\gamma_{1,2}(h)$ is the cross-variogram; N(h) is the point group number at distance h; $Z(X_i)$ is the numerical value at position X_i ; $Z(X_i+h)$ is the numerical value at a distance (X_i+h) ; $Z_1(x_i)$ is the primary variable; $Z_2(x_i)$ is the secondary variable.

$$R^{2} = 1 - \frac{\sum (y_{i} - y_{i}^{*})^{2}}{\sum (y_{i} - \overline{y}_{i})^{2}}$$

$$(3)$$

Where y_i^* is the representation of the estimates, \overline{y}_i is the mean of the measurements y_i .

$$\widehat{Z}_{l} = \sum_{i=1}^{n} \lambda_{i} Z_{l}(x_{i}) + \sum_{j=1}^{p} \lambda_{j} Z_{k}(x_{j})$$

$$(4)$$

Where \widehat{Z}_l is the primary variable to be estimated, Z_l is the primary variable measured, Z_k is the measured secondary variable, x_i and x_j are the known locations, λ_i and λ_j are the weights to be determined.

$$ME = \frac{1}{n} \sum_{i=1}^{n} [Z(X_i) - \widehat{Z}(X_i)], \tag{5}$$

$$RMSE = \sqrt{\frac{\sum_{i=1}^{n} \left[Z(X_i) - \widehat{Z}(X_i) \right]^2}{n}}$$
(6)

Where ME is mean prediction error, RMSE is root mean square prediction error, $Z(X_i)$ is an observed value, $\widehat{Z}(X_i)$ is an estimated value, $\overline{Z}(X_i)$ is the mean of observation values.

Table 3. The performance of R^2

Statistic method		Model performance	
Statistic method	Unacceptable	Acceptable	Good
\mathbb{R}^2	< 0.50	0.50-0.75	> 0.75

regression. Cross-variogram construction and spatial interpolation through cokriging were performed using GS+ version 10.0 (Robertson, 2008). The modeling process involved cross-validation to assess interpolation accuracy and to generate EC_e estimates for the development of spatial distribution maps.

Mapping accuracy

Mapping accuracy refers to the degree of correspondence between predicted values and field-measured observations and is essential for assessing the reliability of spatial interpolation results. In this study, mapping accuracy was evaluated using a cross-validation approach within the cokriging framework. The optimal model performance was determined minimizing the mean error (ME) and root mean square error (RMSE), with ideal values close to zero (Equations 5 and 6) (John et al., 2021). The ME should be close to zero for unbiased approaches, with positive and negative values indicating underestimation and overestimation, respectively (Yao et al., 2014). The RMSE quantifies the accuracy of various prediction methods and should be as small as possible for the best prediction.

RESULTS AND DISCUSSION

Descriptive statistics of EC water ratios

The detailed descriptive statistics measuring the soil electrical conductivity of EC_e from the soil EC water ratios across the three salt-affected soil classes are presented in Table 4. A dilution effect was observed, wherein EC values decreased with increasing soil-to-water ratios. This trend is consistent with earlier findings by Rhoades (1982), Sonmez et al. (2008), and the United States Salinity Laboratory Staff (1954), who reported that greater dilution reduces the measured EC due to lower ion concentrations in the solution.

The CV was used to measure the spatial heterogeneity of soil salinity across all classes. According to Lv et al. (2013), CV is a reliable indicator of variation, with higher values indicating greater regional heterogeneity. In this study, CV values ranged from 0.02 to 3.81 (Table 4), indicating a wide spectrum of variation from weak to strong. In Class 1 (very severely

salt-affected soils), both EC 1:2.5 and 1:5 showed a strong variation, primarily due to the extremely high EC_e values characteristic of this class. In Class 2, the EC 1:2.5 method displayed a weak to moderate degree of variation, while EC 1:5 showed a strong degree of variation, reflecting inconsistent salinity levels ranging from nonsaline to very strongly saline. This variation corresponds with the heterogeneous nature of salinity in this class. Conversely, Class 3 showed the lowest degree of variation across both EC methods, consistent with its classification as nonsaline soil. The reduced CV in Class 3 reflects greater stability and more uniform salinity distribution. Overall, the degree of variation in EC measurements decreased progressively from Classes 1 to 3. These findings provide valuable insights into the spatial behaviour of salinity within salt-affected soil classes and form the basis for subsequent geostatistical modeling and interpretation.

Performance EC_e from EC water ratios of cross-variogram

The performance of the cross-variogram model for estimating EC_e from soil EC water ratios was evaluated using key geostatistical parameters, including R^2 , nugget, sill, range, and nugget:sill ratio (Table 5). Negative spatial correlation between EC_e and EC water ratios were observed in most cases, indicated by negative nugget and sill values (Table 5; Figures 3a to 3f, 3h to 3i, 3m to 3r), while positive correlations were shown in Figures 3g and 3j to 3l.

In Class 1, the Gaussian model provided the best fit for both EC 1:2.5 and EC 1:5 across all sample sizes. The relationships exhibited moderate to strong negative spatial correlations. The Gaussian model explained more than 73% and 76% of the spatial relationship between EC_e and EC water ratios, respectively. The highest estimation accuracy was achieved for EC 1:5 at a sample size of n = 25 ($R^2 = 0.98$), suggesting that smaller sample sizes can provide reliable estimates of EC_e. For EC 1:2.5, the optimal result was found at n = 50, although the R^2 was lower than that for EC 1:5.

In Class 2, the Gaussian model was also identified as the best-fit model for EC 1:2.5, with strong negative correlations for sample sizes

deviation; **Joderate** Moderate Moderate is the standard EC 1:5 (dS Mean Max Min 0.01 0.01 0.01 0.01 0.01 et al. Table 4. Basic statistics from EC water ratios 1:2.5 and 1:5 in different study sites of salt-affected soil classes Degree of on classification from Lv Moderate **Moderate** Strong Weak Weak C0.0030.03 $EC 1:2.5 (dS m^{-1})$ Mean Max Min Moderate Moderate Degree of al. (2017); Strong Strong Strong Mean $EC_e (dS m^{-1})^a$ Max Note: α

Weak Weak n = 50 and 100, while a strong positive correlation was observed for n = 25. For EC 1:5, the Gaussian model was the best fit for n = 50 and 100, while the spherical model was optimal for n = 25. These models explained more than 77% and 85% of the variance in EC_e for EC ratios, respectively. The sample size of n = 25 provided the most accurate estimation in both EC ratios, with EC 1:5 showing slightly higher estimation performance.

Class 3 exhibited high variability in R² values for EC 1:2.5 across different sample sizes, ranging from weak to strong correlations. The highest R^2 (0.81) was observed at n = 50. For EC 1:5, acceptable to strong negative correlations were found, with n = 100 yielding the highest estimation accuracy. Gaussian models were the best fit for both EC water ratios. These models explained more than 76% (EC 1:2.5 at n = 50 and 100) and 65% (EC 1:5) of the spatial variability of EC_e. The relatively weaker correlation in EC 1:2.5 at n = 25 was attributed to lower EC_e values in this class, classified as non-saline.

Analysis of the cross-variogram slopes showed that the slope increased as the EC water ratio decreased, consistent with the dilution effect described by Sonmez et al. (2008). Additionally, cross-variogram slopes decreased from Class 1 to Class 3, reflecting lower EC_e values in less saline soils (Figure 3). Despite stronger correlations in Class 3, the shallow slope indicated limited spatial variability due to low EC_e levels. The results also support previous findings by Phontusang et al. (2017), demonstrating that small sample sizes can provide reliable estimates of EC_e. However, greater consistency and accuracy were observed in larger sample sizes, with sample sizes of 50 and 100 producing stronger and more stable correlations across both EC water ratios (Figure 3; Table 5). This suggests that increased sampling density enhances the reliability of spatial prediction in salt-affected soils.

Additionally, the R² values aligned with results from the one-way ANOVA, which evaluated the relationship between soil EC_e and soil EC water ratios across different sample sizes. The results revealed statistically significant differences $(p \le 0.05)$ across all classes and sample sizes. In Class 1, highly significant differences were observed at sample sizes of 100 and 50 compared to 25 for the 1:2.5 ratio, while for the 1:5 ratio, a sample size of 50 differed significantly from 100 and 25. In Class 2, the sample size of 25 showed a highly significant difference compared to 100 and 50 for the 1:2.5 ratio. For the 1:5 ratio, the sample size of 25 differed significantly from

⁴The 100-number of samples of CV values from each class are from Phontusang et al. (2018)

 $.4 \times 10^{-3}$ $.1 \times 10^{-3}$ 4.9×10^{-4} 4.9×10^{-2} .9×10 Range/Range of influence 45.83 42.08 36.19 0.87 $dS \text{ m}^{-1})^2$ Model Gu g G Table 5. Cross-variogram of EC_e from EC 1:2.5 and 1:5 in different salt-affected soil classes 0.80 31×10^{-3} 3×10^{-3} 2.4×10^{-3} 4.3×10^{-4} 5.0×10^{-4} 4.9×10^{-4} 4.9×10^{-4} 4.9×10^{-4} Range/Range of influence 170.43 322.50 136.83 219.79 140.81 2.01 2.01 Model Gu of EC_e×EC Sample size water ratios 00×100 00×100 50×50

50, with both showing greater significance than the sample size of 100. In Class 3, the sample size of 100 showed a highly significant difference compared to 50, which in turn was more significant than 25 for both EC ratios. These comparisons were further validated using Duncan's post hoc test.

The nugget variance (C_0) represents microscale variability or measurement error (Lv et al., 2013), was generally low and close to zero across most classes and sample sizes, indicating minimal unexplained variability. For the 1:2.5 ratio, nugget values in Classes 1, 2, and 3 were mostly negative and near zero, except for positive, low values at n=25 in Classes 2 and 3. Similarly, for the 1:5 ratio, nugget values were negative and low in Classes 1 and 3, and positive but low in Class 2. These results suggest strong spatial dependence at short distances, indicating a high spatial correlation between EC_e and the EC water ratios.

The sill parameter measures the level of variability in the structure (the maximum variation observed) (Lv et al., 2013). In Class 1, both EC ratios yielded high negative sill values, indicating strong heterogeneity of EC_e derived from EC water ratios. In Class 2, the highest sill values occurred at n = 25 for both EC ratios, possibly due to a high variation in EC_e within this class (Phontusang et al., 2018). Sill values close to zero indicate minimal spatial variability, suggesting that EC water ratios can serve as reliable secondary variables for interpolating EC_e. In Class 3, sill values remained low across all sample sizes for both EC ratios, reflecting a relatively homogeneous salinity distribution.

The range parameter corresponds to the distance which maximum over spatial autocorrelation occurs, indicating the extent of spatial dependence for a given variable (Yang et al., 2011; Lv et al., 2013). In this study, high range values were observed across all classes and for both soil EC water ratios, ranging from 12.81 to 365.28 m, suggesting the presence of a spatial structure (Figure 3). These findings are consistent with previous studies. For instance, Phontusang et al. (2018) reported EC_e range values from 54.70 to 118.20 m using the kriging method in similar study areas, while Yang et al. (2011) reported ranges between 124.2 and 211.8 m. Other studies by Miyamoto et al. (2005) and Yang et al. (2011) also found that salinity distributions exhibited spatial dependence at distances exceeding 100 m. In Class 3, although the range values were high, the relatively low EC_e levels reduced the significance of these ranges, resulting in indistinct

Note: **Gu" is Gaussian; **Sp" is Spherical

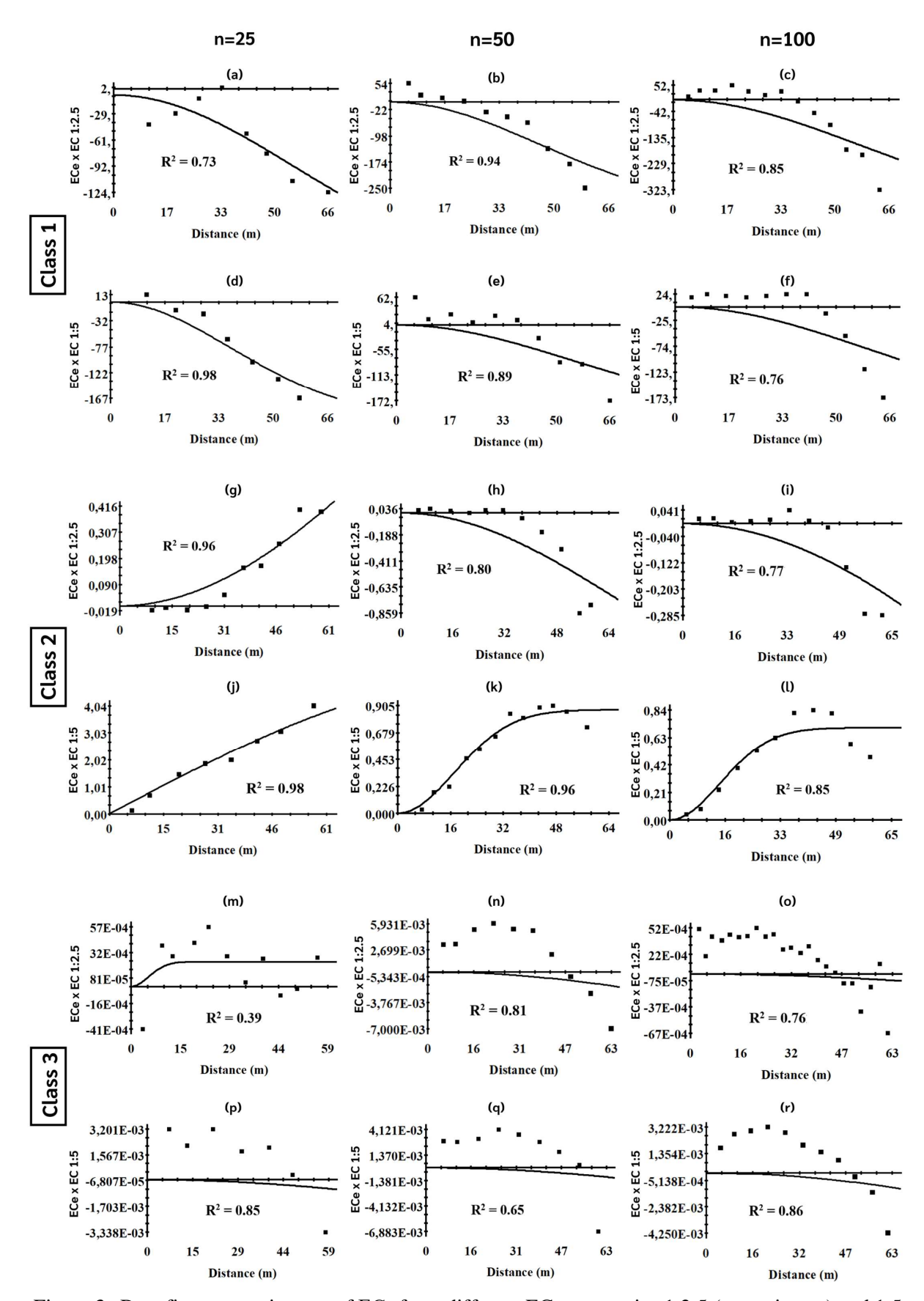


Figure 3. Best-fit cross-variogram of EC_e from different EC water ratios 1:2.5 (a-c, g-i, m-o) and 1:5 (d-f, j-l, p-r) in different salt-affected soil classes

spatial patterns in the respective maps (Figures 4m to 4r).

The nugget:sill ratio measures the level of variability caused by random variables and encompasses the overall spatial heterogeneity (Lv et al., 2013). It serves as a criterion for categorizing the spatial correlation of soil properties in geostatistics. Lower ratios indicate stronger spatial dependence and greater spatial continuity (Cambardella et al., 1994). Across all classes and sample sizes, the nugget:sill ratios for both EC water ratios were low, indicating strong spatial dependence and supporting the use of EC 1:2.5 and EC 1:5 as secondary variables in the interpolation of EC_e. In Class 1, the low ratios for both EC water ratios suggest strongly structured, patchy distributions of EC_e (Figures 4a to 4f), as described by López-Granados et al. (2002). Similarly, Class 2 also exhibited low ratios, indicating strong spatial dependence with moderately patchy distributions (Figures 4g to 4l). In Class 3, despite low nugget:sill ratios indicating strong spatial dependence, the low EC_e values limited the interpretability of spatial variation (Figures 4m to 4r). Overall, the results align with Phontusang et al. (2018), which confirming that spatial variation in salt-affected soils is mainly influenced by structural factors such as topography, hydrological patterns, and climate (Zheng et al., 2009). The spatial dependence of EC_e across study sites is clearly depicted in Figures 3a to 3l. Although Class 3 exhibited the highest range values, particularly for EC 1:5 (up to 365.28 m), the consistently low EC_e values in this class limit the practical relevance of observed spatial structure (Figures 3m to 3r).

Mapping accuracies

The mapping accuracies derived from cokriging are presented in Table 6. Prediction errors were used to evaluate the accuracy of spatial interpolation of soil EC_e using EC measurements at 1:2.5 and 1:5 soil-to-water ratios (Figure 4). According to John et al. (2021), reliable model predictions are indicated by lower ME and RMSE values, ideally close to zero. In this study, the ME values for all classes and sample sizes were generally close to zero for both EC water ratios, indicating that the crossvariogram models were nearly unbiased, with minimal systematic overestimation or underestimation of EC_e.

This study observed that almost all the ME and RMSE values were generally aligned with the corresponding R² values across all classes

and sample sizes (Tables 5 and 6). In Class 1, both positive and negative ME values were observed for EC water ratio 1:2.5 at sample sizes of 25 and 100, respectively, while a negative ME was found at n = 50. A positive ME indicates a slight underestimation of EC_e (i.e., observed > estimated) and a negative ME indicates a slight overestimation of EC_e (i.e., observed < estimated) (Yao et al., 2014). For EC 1:5, negative ME values, indicating a slight overestimation, were observed at sample sizes of 50 and 100, while the smaller sample size of 25 showed a much higher negative ME (-41.29 dS m⁻¹), reflecting severe overestimation. The RMSE values for both EC water ratios in Class 1 ranged from 65.13 to 191.79 dS m⁻¹, indicating considerable prediction errors, which reflect the elevated and highly variable EC_e values observed in this class (0 to 345 dS m⁻¹; Figure 4). According to Rhoades (1982), EC_e values exceeding 12 dS m⁻¹ classify the soil as strongly saline, suggesting that parts of the Muang Pia Sub-district, particularly Class 1, are at high risk of salinity, potentially impacting the productivity of rice and other crops.

In Class 2, ME values for both EC ratios were close to zero, indicating minimal bias in the estimation models. The RMSE values were low (≤ 2.30 dS m⁻¹), suggesting high predictive accuracy. In Class 3, ME values were also close to zero, with slight overestimation observed only at sample sizes of 100 (for EC 1:2.5) and 25 (for EC 1:5). RMSE values for both EC ratios were very low (≤ 0.33 dS m⁻¹), reflecting high estimation accuracy. However, in Class 3, the low ME and RMSE values for EC 1:2.5 at n = 25 were not aligned with the low R², likely because the low EC₆ values in this non-saline zone.

A comparison of RMSE values across the three classes showed that Class 1 consistently produced higher RMSE than Classes 2 and 3, a result that aligns with Phontusang et al. (2018). This is attributed to higher EC_e values and a greater CV (> 2) in Class 1 (Table 4). The elevated RMSE may also be influenced by limited EC_e contrast, where a narrow range of EC_e values (e.g., EC_e CV = 0.03 in Table 4) reduce spatial differentiation, thereby reducing model accuracy.

Cokriging interpolation using EC water ratios of 1:2.5 and 1:5 as secondary variables yielded the highest estimation performance for EC_e. This improvement is attributable to the strong correlation between EC_e and the EC water ratios, as reflected in the fitted cross-variogram models (Bogunovic et al., 2017; Wu et al., 2025).

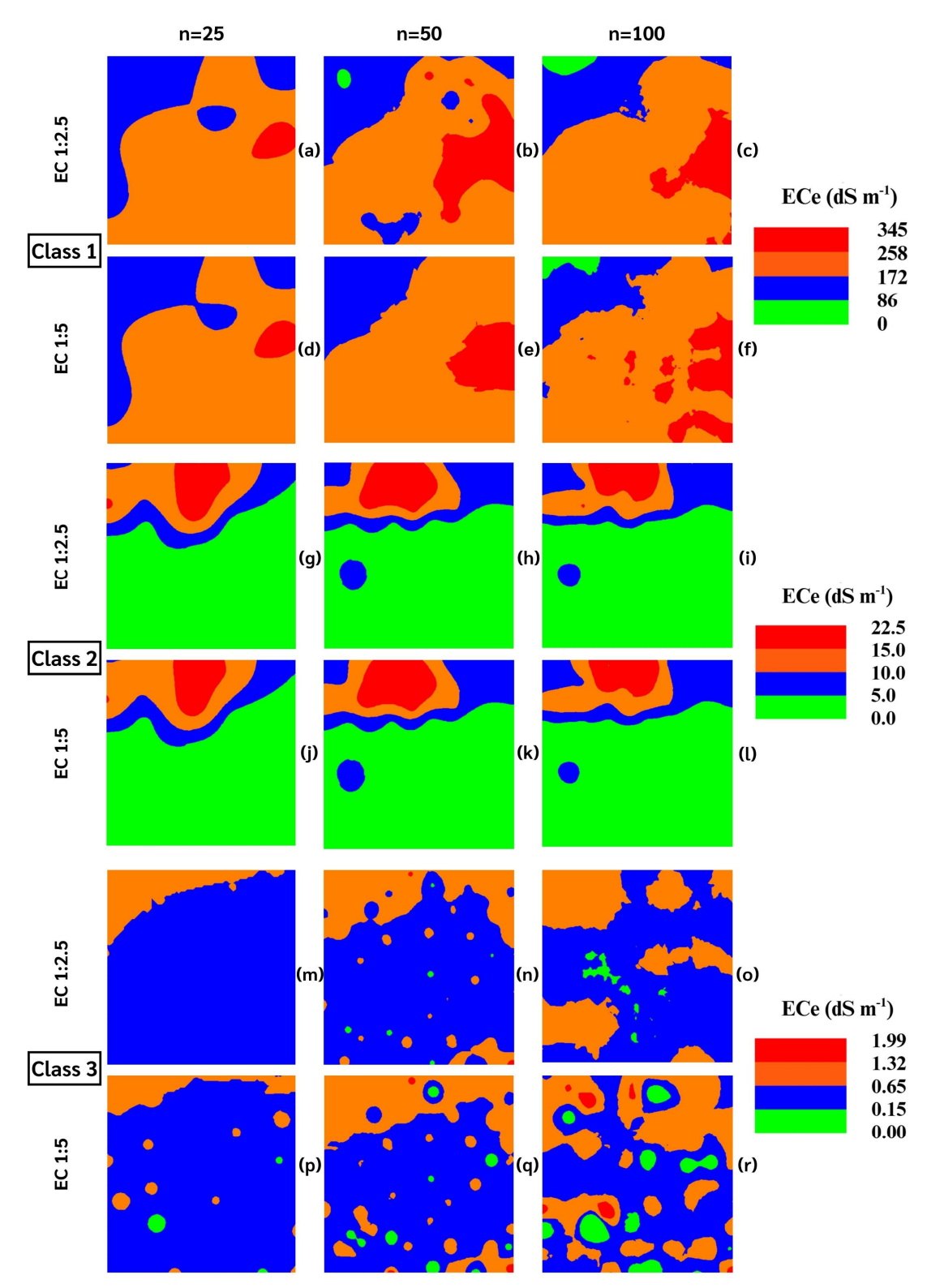


Figure 4. Maps of cokriging estimations from different EC water ratios 1:2.5 (a-c, g-i, m o) and 1:5 (d-f, j-l, p-r) in different salt-affected soil classes

Cokriging has been shown to outperform ordinary kriging when a strong relationship exists between primary and secondary variables, especially when the primary variable is difficult or costly to measure. In such cases, cokriging enables the use of readily obtainable secondary data to enhance

spatial prediction accuracy (Wu et al., 2025). This approach also reduces sampling effort and cost (Xie and Li, 2016). However, cokriging inherently smooths spatial variability, which may obscure local heterogeneity. Furthermore, incorporating multiple secondary variables

Class	Sample size of	ME 1:2.5	RMSE 1:2.5	ME 1:5	RMSE 1:5
	EC _e ×EC water ratios	$(dS m^{-1})$	$(dS m^{-1})$	$(dS m^{-1})$	$(dS m^{-1})$
1	25×25	3.06	72.25	-41.29	191.79
	50×50	-0.41	65.17	-0.46	65.13
	100×100	2.68	69.70	-0.14	68.30
2	25×25	0.03	2.25	0.01	2.30
	50×50	0.00	0.78	0.01	0.78
	100×100	0.02	1.16	0.02	1.31
3	25×25	0.00	0.17	-0.05	0.16
	50×50	0.00	0.33	0.01	0.24
	100×100	-0.02	0.11	0.06	0.23

Table 6. Accuracies of cokriging maps generated from EC water ratios to estimate EC_e

increases model complexity and uncertainty due to the need to estimate more parameters (Knotters et al., 1995; Wang et al., 2012).

In terms of estimated EC_e ranges, Phontusang et al. (2018) ranging between 65 to 368, 0 to 25, and 0 to 3.7 dS m⁻¹ for Classes 1, 2, and 3, respectively. In this study, the estimated EC_e values ranged between 0 to 345 (Class 1), 0 to 22.5 (Class 2), and 0 to 1.99 dS m⁻¹ (Class 3) (Figure 4). These results demonstrate that EC_e predictions based on EC water ratios of 1:2.5 and 1:5 are in close agreement with field-measured values reported by Phontusang et al. (2018). This confirms the suitability of EC water ratios as effective secondary variables for cokriging-based estimation of soil EC_e .

CONCLUSIONS

This study demonstrates that EC_e can be accurately estimated using EC 1:2.5 and 1:5 ratios with cokriging spatial interpolation, supported by strong correlations (R2 up to 0.98) and generally low ME and RMSE values. While the EC 1:5 ratio with Gaussian models performed well for most classes, Class 1 (n = 25) exhibited higher errors. The approach provides an effective spatial interpolation method for the study area, reflecting the strong site-specific co-dependence between EC water ratios and EC_e. While its applicability to other regions requires external validation, this approach complements, rather than replaces, traditional saturated paste extraction, and support precision agriculture and sustainable management of salt-affected soils.

ACKNOWLEDGEMENT

The authors would like to acknowledge the ASEAN and GMS Countries Scholarship 2023 (Grant number: KKU ASEAN-GMS 027/2024), Khon Kaen University, Thailand, for the support of the master program.

REFERENCES

Abdelaal, S. M. S., Moussa, K. F., Ibrahim, A. H., Mohamed, E. S., Kucher, D. E., & Al-Faraj, M. K. (2021). Mapping spatial management zones of salt-affected soils in arid region: A case study in the east of the Nile Delta, Egypt. *Agronomy*, 11(12), 2510. https://doi.org/10.3390/agronomy11122510

Bogunovic, I., Pereira, P., & Brevik, E. C. (2017). Spatial distribution of soil chemical properties in an organic farm in Croatia. *Science of the Total Environment*, 584–585, 535–545. https://doi.org/10.1016/j.scitotenv.2017.01. 062

Cambardella, C. A., Moorman, T. B., Novak, J. M., Parkin, T. B., Karlen, D. L., Turco, R. F., & Konopka, A. E. (1994). Field-scale variability of soil properties in Central Iowa soils. *Soil Science Society of America Journal*, 58(5), 1501–1511. https://doi.org/10.2136/sssaj1994.03615995005800050033x

Chi, C. M., & Wang, Z-C. (2009). Characterizing salt-affected soils of Songnen Plain using saturated paste and 1:5 soil-to-water extraction methods. *Arid Land Research and Management*, 24(1), 1–11. https://doi.org/10.1080/15324980903439362

Clark, I., & Harper, W. V. (2007). Practical geostatistics. *Journal of the Royal Statistical Society. Series A (General)*, 144(4), 537. https://doi.org/10.2307/2981833

Corwin, D. L., & Yemoto, K. (2020). Salinity: Electrical conductivity and total dissolved solids. *Soil Science Society of America Journal*, 84(5), 1442–1461. https://doi.org/10.1002/saj2.20154

Daneshvar, S., Mosaddeghi, M. R., & Afyuni, M. (2024). Effect of biochar and hydrochar of

- pistachio residues on physical quality indicators of a sandy loam soil. *Geoderma Regional*, *36*, e00740. https://doi.org/10.1016/j.geodrs.2023.e00740
- Gee, G. W., & Or, D. (2002). 2.4 particle-size analysis. *Methods of Soil Analysis: Part 4 Physical Methods*, 5.4, pp. 255–293. Madison, WI: Soil Science Society of America. https://doi.org/10.2136/sssabookser5.4.c12
- Goovaerts, P. (1997). Geostatistics for natural resources evaluation. New York: Oxford University Press. https://doi.org/10.1093/oso/9780195115383.001.0001
- Gozukara, G., Altunbas, S., Dengiz, O., & Adak, A. (2022). Assessing the effect of soil to water ratios and sampling strategies on the prediction of EC and pH using pXRF and Vis-NIR spectra. *Computer and Electronics in Agriculture*, 203(11), 107459. https://doi.org/10.1016/j.compag.2022.107459
- He, Y., DeSutter, T., Hopkins, D., Jia, X., & Wysocki, D. A. (2013). Predicting EC_e of the saturated paste extract from value of EC1:5. *Canadian Journal of Soil Science*, *93*(5), 585–594. https://doi.org/10.4141/CJSS2012-080
- He, Y., DeSutter, T., Prunty, L., Hopkins, D., Jia, X., & Wysocki, D. A. (2012). Evaluation of 1:5 soil to water extract electrical conductivity methods. *Geoderma*, 185–186, 12–17. https://doi.org/10.1016/j.geoderma.2012.03. 022
- Hossen, B., Yabar, H., & Faruque, M. J. (2022). Exploring the potential of soil salinity assessment through remote sensing and GIS: Case study in the coastal rural areas of Bangladesh. *Land*, *11*(10), 1784. https://doi.org/10.3390/land11101784
- Iwai, C. B., Oo, A. N., & Topark-ngarm, B. (2012). Soil property and microbial activity in natural salt affected soils in an alternating wetdry tropical climate. *Geoderma*, 189–190, 144–152. https://doi.org/10.1016/j.geoderma. 2012.05.001
- John, K., Agyeman, P. C., Kebonye, N. M., Isong, A. I., Ayito, E. O., & Ofem, K. I. (2021). Hybridization of cokriging and gaussian process regression modelling techniques in mapping soil sulphur. *Catena*, 206, 105534. https://doi.org/10.1016/j.catena.2021.105534
- Kargas, G., Londra, P., & Sgoubopoulou, A. (2020). Comparison of soil EC values from

- methods based on 1:1 and 1:5 soil to water ratios and ECe from saturated paste extract based method. *Water*, *12*(4), 1010. https://doi.org/10.3390/W12041010
- Khanh, P. T., Pramanik, S., & Ngoc, T. T. H. (2024). Soil permeability of sandy loam and clay loam soil in the paddy fields in An Giang Province in Vietnam. *Environmental Challenges*, 15, 100907. https://doi.org/10.1016/j.envc.2024.100907
- Knotters, M., Brus, D. J., & Oude Voshaar, J. H. (1995). A comparison of kriging, co-kriging and kriging combined with regression for spatial interpolation of horizon depth with censored observations. *Geoderma*, 67(3–4), 227–246. https://doi.org/10.1016/0016-7061(95)00011-C
- Leksungnoen, N., Andriyas, T., & Andriyas, S. (2018). ECe prediction from EC_{1:5} in inland salt-affected soils collected from Khorat and Sakhon Nakhon basins, Thailand. *Communications in Soil Science and Plant Analysis*, 49(21), 2627–2637. https://doi.org/10.1080/00103624.2018.1524900
- Li, J., Pu, L., Han, M., Zhu, M., Zhang, R., & Xiang, Y. (2014). Soil salinization research in China: Advances and prospects. *Journal of Geographical Sciences*, 24(5), 943–960. https://doi.org/10.1007/s11442-014-1130-2
- Li, L., Lu, J., Wang, S., Ma, Y., Wei, Q., Li, X., & Cong, R. (2016). Methods for estimating leaf nitrogen concentration of winter oilseed rape (*Brassica napus* L.) using in situ leaf spectroscopy. *Industrial Crops and Products*, 91, 194–204. https://doi.org/10.1016/j.indcrop.2016.07.008
- López-Granados, F., Jurado-Expósito, M., Atenciano, S., García-Ferrer, A., Sánchez De La Orden, M., & García-Torres, L. (2002). Spatial variability of agricultural soil parameters in southern Spain. *Plant and Soil*, 246(1), 97–105. https://doi.org/10.1023/A:1021568415380
- Lv, Z. Z., Liu, G. M., Yang, J. S., Zhang, M. M., & He, L. D. (2013). Spatial variability of soil salinity in Bohai Sea coastal wetlands, China: Partition into four management zones. *Plant Biosystem*, *147*(4), 1201–1210. https://doi.org/10.1080/11263504.2013.861531
- Marchetti, A., Piccini, C., Francaviglia, R., & Mabit, L. (2012). Spatial distribution of

- soil organic matter using geostatistics: A key indicator to assess soil degradation status in Central Italy. *Pedosphere*, 22(2), 230–242. https://doi.org/10.1016/S1002-0160(12) 60010-1
- Matthees, H. L., He, Y., Owen, R. K., Hopkins, D., Lee, J., Clay, D. E., ... & Malo, D. D. (2017). Predicting soil electrical conductivity of the saturation extract from a 1:1 soil to water ratio. *Communications in Soil Science and Plant Analysis*, 48(18), 2148–2154. https://doi.org/10.1080/00103624.2017. 1407780
- Mitsuchi, M., Wichaidit, P., & Jeungnijnirund, S. (1986). *Outline of soils of the northeast plateau, Thailand: Their characteristics and constraints*. Technical paper, No. 1, pp. 80. Khon Kaen Province, Thailand: Agricultural Development Research Center in Northeast. Retrieved from https://books.google.co.id/books/about/Outline_of_Soils_of_the_Northeast_Platea.html?id=-n4_AAAAYAAJ&redir_esc=y
- Miyamoto, S., Chacon, A., Hossain, M., & Martinez, I. (2005). Soil salinity of urban turf areas irrigated with saline water: I. Spatial variability. *Landscape and Urban Planning*, 71(2–4), 233–241. https://doi.org/10.1016/j.landurbplan.2004.03.006
- Muang Pia Sub-district. (2022). *Muang Pia Subdistrict Administration Organization*. Retrieved from https://www.muangpere.go.th/data.php?content_id=2
- Or, Y. M. (2010). *A study in determining the sample size in geostatistics*. Alberta, Canada: University of Alberta. https://doi.org/10.7939/R3SC96
- Phontusang, P., Katawatin, R., Pannangpetch, K., & Lerdsuwansri, R. (2017). Sampling strategies for geostatistical analyses of field-scale spatial variability of electrical conductivity in inland salt-affected soils. *International Journal of Geoinformatics*, 13(2), 71–84. Retrieved from https://journals.sfu.ca/ijg/index.php/journal/article/view/1036
- Phontusang, P., Katawatin, R., Pannangpetch, K., Lerdsuwansri, R., Kingpaiboon, S., & Wongpichet, K. (2018). Field-scale spatial variability of electrical conductivity of the inland, salt-affected soils of Northeast Thailand. Walailak Journal of Science and

- *Technology*, *15*(5), 341–355. https://doi.org/10.48048/wjst.2018.3474
- Plaster, E. J. (2013). Soil Science and Management. Boston: Cengage Learning. Retrieved from https://books.google.co.th/books?id=zeoWAAAQBAJ
- Qadir, M., Noble, A. D., Schubert, S., Thomas, R. J., & Arslan, A. (2006). Sodicity-induced land degradation and its sustainable management: Problems and prospects. *Land Degradation and Development*, 17(6), 661–676. https://doi.org/10.1002/ldr.751
- Qi, W., Zhang, Z., Wang, C., & Huang, M. (2021). Prediction of infiltration behaviors and evaluation of irrigation efficiency in clay loam soil under Moistube® irrigation. *Agricultural Water Management*, 248, 106756. https://doi.org/10.1016/j.agwat.2021.106756
- Rhoades, J. D. (1982). Soluble salts. *Methods of Soil Analysis: Part 2 Chemical and Microbiological Properties*, 9.2.2, Second Edition, pp.167–179. https://doi.org/10.2134/agronmonogr9.2.2ed.c10
- Robertson, G. P. (2008). *GS+: Geostatistics for Environmental Scientists, Second Edition.* https://doi.org/10.1002/9780470517277.index
- Rukadi, K., Phontusang, P., & Sriprachote, A. (2025). Soil ECe prediction from different EC water ratio and sample sizes in salt-affected soils. *EnvironmentAsia*, 18(2), 121–130. https://doi.org/10.14456/ea.2025.42
- Sankla, N., Loutchanwoot, P., Khankhum, S., Khammuang, S., Sarnthima, R., & Sunthamala, N. (2022). *In vitro* antioxidant and immunological-associated activities of ethanol extracts of *Azima sarmentosa* (Blume) Benth. and Hook. F. *Tropical Journal of Natural Product Research*, 6(12), 2007–2013. https://doi.org/10.26538/tjnpr/v6i12.18
- Seo, B-S., Jeong, Y-J., Baek, N-R., Park, H-J., & Yang, H. I. (2022). Soil texture affects the conversion factor of electrical conductivity from 1:5 soil—water to saturated paste extracts. *Pedosphere*, 32(6), 905–915. https://doi.org/10.1016/j.pedsph.2022.06.023
- Shahid, S. A., Zaman, M., & Heng, L. (2018). Introduction to soil salinity, sodicity and diagnostics techniques. Guideline for Salinity Assessment, Mitigation and Adaptation Using Nuclear and Related Techniques. Springer,

- Cham. https://doi.org/10.1007/978-3-319-96190-3_1
- Smagin, A., Kacimov, A., & Sokolov, N. (2024). EC conversion for 1:5 extracts and standard saturated soil—water pastes in the assessment of arid land salinization: Classical methodologies revisited. *Journal of the Saudi Society of Agricultural Sciences*, 23(4), 277–288. https://doi.org/10.1016/j.jssas.2023.12.005
- Sonmez, S. C., Buyuktas, D., & Okturen, F. (2008). Assessment of different soil to water ratios (1:1, 1:2.5, 1:5) in soil salinity studies. *Geoderma*, 144(1–2), 361–369. https://doi.org/10.1016/j.geoderma.2007.12.005
- Spielvogel, S., Prietzel, J., & Kögel-Knabner, I. (2016). Stand scale variability of topsoil organic matter composition in a high-elevation Norway spruce forest ecosystem. *Geoderma*, 267, 112–122. https://doi.org/10.1016/j.geoderma.2015.12.001
- Sukchan, S. (2005). Salt-affected soil map of Thung Kula Ronghai at 1:50,000 scale (in Thai). *Office of Soil Survey and Land Use Plannning*, Bangkok: 12–4. Retrieved from https://scholar.google.co.id/scholar?cluster=1 3698091492948044411&hl=id&as_sdt=2005 &sciodt=0,5
- Thanh, N. N., Chotpantarat, S., Trung, N. H., Ngu, N. H., & Muoi, L. V. (2022). Mapping groundwater potential zones in Kanchanaburi Province, Thailand by integrating of analytic hierarchy process, frequency ratio, and random forest. *Ecological Indicators*, 145, 109591. https://doi.org/10.1016/j.ecolind. 2022.109591
- United States Salinity Laboratory Staff. (1954). Diagnosis and improvement of saline and alkaline soils. *Agricultural Handbook no. 60*, pp. 83–88. Washington DC, USA: United States Department of Agriculture. Retrieved from https://www.ars.usda.gov/ARSUser Files/20360500/hb60_pdf/hb60complete.pdf
- Wang, K., Zhang, C., & Li, W. (2012). Comparison of geographically weighted regression and regression kriging for estimating the spatial distribution of soil organic matter. *GIScience & Remote Sensing*, 49(6), 915–932. https://doi.org/10.2747/1548-1603.49.6.915

- Weather and Climate. (2025). Ban Phai rainfall & precipitation: Monthly Averages and yearround insights. Retrieved from https://weather-and-climate.com/averagemonthly-precipitation-Rainfall,ban-phaikhon-kaen-province-th,Thailand
- Webster, R., & Oliver, M. A. (2007). *Geostatistics* for environmental scientists, 2nd ed. Chichester, UK: John Wiley and Sons, Ltd. https://doi.org/10.1002/9780470517277
- Wichaidit, P. (1995). Report in survey and studies of salt-affected soils: Khon Kaen Province (in Thai). *Soil Survey and Classification*, 1–20. Retrieved from https://scholar.google.co.id/scholar?cites=13485481174742532267&as_sdt=2005&sciodt=0,5&hl=id
- Wu, X., Jiang, N., Li, A., Yang, Y., & Cheng, H. (2025). Spatial distribution pattern of soil organic matter in the wind erosion region of northeastern China based on the cokriging method. *Catena*, 248, 108575. https://doi.org/ 10.1016/j.catena.2024.108575
- Xie, X-L., & Li, A-B. (2016). Improving spatial estimation of soil organic matter in a subtropical hilly area using covariate derived from vis-NIR spectroscopy. *Biosystems Engineering*, *152*, 126–137. https://doi.org/10.1016/j.biosystemseng.2016.06.007
- Yang, B., Liu, H., Kang, E. L., Shu, S., Xu, M., Wu, B., ... & Yu, B. (2021). Spatio-temporal cokriging method for assimilating and downscaling multi-scale remote sensing data. *Remote Sensing of Environment*, 255, 112190. https://doi.org/10.1016/j.rse.2020. 112190
- Yang, F., Zhang, G., Yin, X., & Liu, Z. (2011). Field-scale spatial variation of saline–sodic soil and its relation with environmental factors in Western Songnen Plain of China. *International Journal of Environmental Research and Public Health*, 8(2), 374–387. https://doi.org/10.3390/ijerph8020374
- Yao, R. J., Yang, J. S., Gao, P., Shao, H. B., Liu, G. M., & Yu, S. P. (2014). Comparison of statistical prediction methods for characterizing the spatial variability of apparent electrical conductivity in coastal salt-affected farmland. *Environmental Earth Sciences*, 71(1), 233–243. https://doi.org/10.1007/s12665-013-2427-7

- Yates, S. R., & Warrick, A. W. (2002). Geostatistics. Methods of Soil Analysis. Part 4 Physical Methods. *Soil Science Society of America*, Madison, WI. pp. 81–118. https://doi.org/10.2136/sssabookser5.4.c5
- Zheng, Z., Zhang, F., Ma, F., Chai, X., Zhu, Z., Shi, J., & Zhang, S. (2009). Spatiotemporal changes in soil salinity in a drip-irrigated field. *Geoderma*, 149(3–4), 243–248. https://doi.org/10.1016/j.geoderma.2008.12.002